Journal of Chromatography A, 1218 (2011) 5542–5548

Contents lists available at ScienceDirect

Journal of Chromatography A

journal homepage: www.elsevier.com/locate/chroma

Fabrication of graphene/poly(methyl methacrylate) composite electrode for capillary electrophoretic determination of bioactive constituents in *Herba Geranii*

Xia Wang[a,b], Jiyang Li[a], Weidong Qu[b], Gang Chen[a,*]

[a] School of Pharmacy, Fudan University, 826 Zhangheng Road, Shanghai 200032, China
[b] Key Laboratory of Public Health and Safety, Ministry of Education, School of Public Health, Fudan University, 826 Zhangheng Road, Shanghai 200032, China

ARTICLE INFO

Article history:
Received 9 April 2011
Received in revised form 2 June 2011
Accepted 7 June 2011
Available online 17 June 2011

Keywords:
Graphene
Poly(methyl methacrylate)
Composite electrode
Capillary electrophoresis
Amperometric detection
Herba Geranii

ABSTRACT

This report describes the development and application of a novel graphene/poly(methyl methacrylate) composite electrode as a sensitive amperometric detector of capillary electrophoresis. The composite electrode was fabricated on the basis of the in situ polymerization of a mixture of graphene and prepolymerized methyl methacrylate in the microchannel of a piece of fused silica capillary under heat. SEM, XRD and FT-IR offered insights into the nature of the composite. The results indicated that graphenes were well dispersed in the composite to form an interconnected conducting network. The performance of this unique graphene-based detector has been demonstrated by separating and detecting seven naturally occurring phenolic compounds in *Herba Geranii* in combination with capillary electrophoresis. The graphene-based detector offered significantly lower operating potentials, substantially enhanced signal-to-noise characteristics, and lower expense of operation. The simplicity and significant performance exhibited by the graphene/poly(methyl methacrylate) composite electrode also indicate great promise for microchip CE, flowing injection analysis, and other microfluidic analysis systems.

1. Introduction

Graphene has attracted more and more attention because of its unique nanostructure and properties [1–3]. As an important two-dimension nanomaterial, graphene has been employed to fabricate electrochemical sensors and biosensors because of its excellent conductivity and electrocatalytic activity [4–7]. The existing approaches to producing graphene include mechanical exfoliation, chemical vapor deposition, and chemical or thermal reduction of graphite oxide (GO). Among them, the last approach is considered to be the most economical way to produce graphene. Usually, graphite powder was oxidized with some strong oxidants and exfoliated to form GO that was further reduced to graphene [2]. Recently, Martin et al. demonstrated that the use of GO as electrochemical detector in microfluidics was of no advantage in terms of sensitivity or selectivity over that of graphite microparticles [8]. It might be attributed to the low electrical conductivity of GO. In comparison, it was demonstrated that electrically conductive graphene showed strong electrocatalytic activity when it was employed to improve the electrochemical response of some bioactive substances [9–12]. The ability of graphene to promote the electron-transfer reactions suggests great promise for the sensitive amperometric detection of capillary electrophoresis (CE).

Since CE in its modern form was first described by Jorgenson and Lukacs [13,14], it has been applied in the separation and determination of a variety of samples because of its minimal sample volume requirements, short analysis time, and high separation efficiency. It holds considerable promise for biomedical and pharmaceutical analysis, clinical diagnostics, environmental monitoring, and forensic investigations [15–19]. Amperometric detection (AD) offers great promise for CE, with features that include high sensitivity, inherent miniaturization of the detector and control instrumentation, low cost, low-power demands, and high compatibility with micromachining technologies [20]. The performance of CE–AD is strongly influenced by the detection-electrode material. Usually, the detection electrode should provide favorable sensitivity and reproducibility. To date, a wide range of carbon-based materials, including graphite, carbon nanotube (CNT), graphene, and boron-doped diamond, have been employed to fabricate the detection electrodes of CE [12,21,19]. Among them, the most commonly used detection electrodes of CE were fabricated using graphite [19]. Recently, a variety of CNT-based electrodes were developed for the amperometric detection of CE. They included CNT modified screen-printed carbon electrode [22,23], CNT/alginate composite modified electrode [24], CNT/epoxy composite electrode [25], CNT/cellulose composite modified electrode [26], CNT/poly(urea-formaldehyde) composite electrode [27], etc. More recently, a novel

* Corresponding author. Tel.: +86 21 5198 0061; fax: +86 21 6564 1740.
E-mail address: gangchen@fudan.edu.cn (G. Chen).

0021-9673/$ – see front matter © 2011 Elsevier B.V. All rights reserved.
doi:10.1016/j.chroma.2011.06.034

graphene/poly(urea-formaldehyde) composite modified electrode was developed as a sensitive amperometric detector CE. The electrode was fabricated on the basis of the polycondensation of a mixture of graphene and urea-formaldehyde prepolymer on the surface of a platinum disk electrode [12]. In addition, boron-doped diamond electrodes had been also been applied in the amperometric detection of CE [28]. They exhibited very attractive electrochemical properties, such as low and stable background currents, a wide potential window in aqueous media, minimized adsorption of most organic substances, long-term stability of the response, and high sensitivity [21].

Traditional Chinese herbal medicine, *Herba Geranii* is the dried overground part of *Geranium carolinianum* L. It has been widely used to treat rheumatism, muscle soreness, numbness, diarrhea, and dysentery [29]. The major bioactive constituents in it include rutin, hyperin, kaempferol, corilagin, geraniin, gallic acid, protocatechuic acid, etc. Their contents are important parameters for evaluating the quality of the herbal drug. Hence, it is necessary to establish some rapid, simple, and accurate approaches for the determination of the bioactive constituents in *Herba Geranii*. Liquid chromatography has been widely employed in the simultaneous determination of bioactive constituents in it [30]. Usually, the content of the constituents in the herbal drugs is very low. Highly sensitive detection approaches are highly demanded. Because the naturally occurring phenolic constituents mentioned above contain phenolic hydroxyl groups that are electroactive at modest oxidation potential, CE coupled with highly sensitive graphene-based detection electrode should be a useful technique for the constituent investigation of *Herba Geranii*.

Poly(methyl methacrylate) (PMMA) is a versatile polymer with the features of its versatile chemical properties, low price, excellent optic transparency, and satisfactory mechanical strength [31,32]. Graphene/PMMA composites have been prepared by solvent evaporation [33,34]. However, the content of graphene in the composite was less than 1% (w/w). The electric conductivity of the prepared composite was low and not suitable for the fabrication of electrodes.

To solve the problem, a novel method based on the in situ polymerization of a mixture of graphene and prepolymerized methyl methacrylate was developed for the fabrication of graphene/PMMA composite microdisc electrode in this work. The content of graphene in the composite was increased to 25% (w/w) so that the electric conductivity of the prepared composite was significantly enhanced. To the best of our knowledge, there is no earlier report on the preparation of graphene/PMMA composite electrode by in situ polymerization for electrochemical sensing. The prepared graphene-based electrode was employed as a sensitive amperometric detector of a CE system. The fabrication details, characterization, feasibility, and performance of the novel graphene/PMMA composite electrode have been demonstrated by detecting seven phenolic compounds in *Herba Geranii* in connection with CE in the following sections.

2. Experimental

2.1. Reagents and solutions

Rutin, hyperin, corilagin, gallic acid, and protocatechuic acid were purchased from National Institute for the Control of Pharmaceutical and Biological Products (Beijing, China) while kaempferol and geraniin were supplied by Shanghai Tauto Biotech Co., Ltd. (Shanghai, China). Methyl methacrylate (MMA), 2-2′-azo-bis-isobutyronitrile (AIBN), borax, graphite powder, sodium nitrate, potassium permanganate, hydrogen peroxide solution (30%, w/w), hydrazine hydrate (85%, w/w), and sulfuric acid (98%, w/w) were all supplied by SinoPharm (Shanghai, China). All aqueous solutions were made up in doubly distilled water. Other chemicals were of analytical grade.

Stock solutions of rutin, hyperin, kaempferol, corilagin, and geraniin (1 mg/mL) were all prepared in methanol while the stock solutions of gallic acid and protocatechuic acid (2 mg/mL) were made in doubly distilled water.

2.2. Preparation of graphene

GO was synthesized from graphite by a modified Hummers method [35]. Briefly, 2 g graphite powder was dispersed in 46 mL of sulfuric acid (98%, w/w) under agitation. Subsequently, 1.2 g sodium nitrate and 6 g potassium permanganate were successfully added into the mixture in an ice bath. Note that both compounds should be added slowly to prevent the temperature from exceeding 20 °C. After the reaction was allowed to proceed in a 35 °C water bath for 30 min, 92 mL of doubly distilled water was gradually added. And then, the temperature of the water bath was increased to 98 °C and the reaction was maintained for 40 min in order to increase the oxidation degree of the GO product. After the volume of the resultant suspension was adjusted to 280 mL with doubly distilled water, 6 mL of hydrogen peroxide solution (30%, w/w) was added while the color of the suspension changed from brown to bright-yellow. The prepared GO could be easily isolated from the solution by vacuum filtration. The sulfuric acid and salt impurities in the crude GO were removed by washing with 5% (w/w) hydrochloric acid, 1% (w/w) hydrochloric acid, and doubly distilled water successively with the aid of vacuum filtration. The wet GO was dewatered by vacuum drying (50 °C).

To prepare graphene, 50 mg GO powder was dispersed in 50 mL doubly distilled water and sonicated in an ultrasonic cleaner (SKQ-2200, frequency 56 kHz, output power 100 W) for 1 h. Reduction of GO was carried out by adding 0.3 mL hydrazine hydrate (85%, w/w) into the solution. The reduction reaction was allowed to take place at 95 °C for 1 h. The obtained black graphene could be easily isolated form the solution by vacuum filtration and was purified by washing with copious amounts of doubly distilled water. Finally, it was washed with absolute ethanol and dried in vacuum.

2.3. Electrode fabrication

Prior to the fabrication, 0.04 g of AIBN was dissolved in 20 mL of MMA and the clear mixed solution in a conical flask was allowed to prepolymerize to generate a dense prepolymer solution in an 85 °C water bath for ~15 min under nitrogen flow. The prepared viscous prepolymerized MMA solution was hand-mixed with graphene powder in a ratio of 3:1 (w/w). Subsequently, a piece of copper wire (10 cm long, 150 μm diameter) was inserted into a 3.0 cm long fused silica capillary (320 μm I.D. × 450 μm O.D., Hebei Yongnian Ruipu Chromatogram Equipment Co., Ltd., Hebei, China) and a 2 mm opening was left in the capillary for the subsequent filling of the mixture of the prepolymerized MMA and graphene powder. The mixture was then packed into the capillary by pressing the opening end of the capillary (to a depth of ~3 mm) into a sample of the composite. The graphene-containing mixture should touch the end of the copper wire inside the capillary tightly for the electric contact and was then allowed to polymerize completely in a 45 °C oven for 10 h. Finally, hot melt adhesive was applied to the open end of the capillary to glue the copper wire in place. The graphene-filled end of the electrode was successively polished with emery paper to form a disc electrode. In addition, a graphite/PMMA composite electrode, used for comparison, was prepared in the same procedures.

2.4. Apparatus

The CE–AD system used in this work has been described in our previous report [24]. A ±30 kV high-voltage dc power supply (Shanghai Institute of Nuclear Research, China) provided a separation voltage between the two ends of the capillary. The inlet of the capillary was held at a positive potential while the outlet of capillary was maintained at ground. The separations were carried out in a 40 cm length of 25 μm I.D. and 360 μm O.D. fused silica capillary (Polymicro Technologies, Phoenix, AZ, USA). A three-electrode electrochemical cell consisting of a disc detection electrode, a platinum auxiliary electrode and an Ag/AgCl wire as the reference electrode, was used in combination with a BAS LC-4 C amperometric detector (Bioanalytical Systems Inc., West Lafayette, IN, USA) for the detection of CE. The composite detection electrode was positioned carefully opposite the outlet of the capillary with the aid of a high-integrated 3-D amperometric setup and arranged in a wall-jet configuration. The gap between the end of the capillary and the surface of the detection electrode was ~50 μm. The details and operation procedure of the 3-D adjustable alignment device can be found in our previous report [24].

The surface morphology of PMMA sheet, graphenes, and the cross sections of graphene/PMMA and graphite/PMMA composites were observed by scanning electron microscope (PHILIPS XL 30). Thermogravimetric analysis (TGA) and differential TGA (DTGA) were made with a Perkin Elemer Pyris 1 DTA–TGA instrument in air at a heating rate of 10 °C/min. X-ray diffraction (XRD) measurements were carried out using a Rigaku D/max-rB diffractometer (Rigaku, Tokyo, Japan) with CuK-α1 radiation (40 kV, 60 mA). The Fourier transform infrared spectroscopy (FT-IR) spectra of GO, graphene, PMMA, and graphene/PMMA composite were measured using a FT-IR spectrometer (NEXUS470, NICOLET).

2.5. Sample preparation

A sample of *Herba Geranii* (an herbal drug) was obtained from Yang-He-Tang Traditional Chinese Medicine Store (Shanghai, China). It was dried at 60 °C for 2 h and then was pulverized. About 2.0 g of the powder was weighed accurately and dispersed in 50 mL of methanol. The mixture was kept in a 60 °C water bath for 3 h. After cooling, it was sonicated for 30 min and filtered through a filter paper. The residue was washed twice with 10 mL of methanol. The extract and washings were combined and the solvent in the mixture was removed under vacuum. The obtained residue was then dissolved in 10 mL of 50 mM borate buffer (pH 9.2, running buffer) for the subsequent CE analysis.

2.6. CE procedures

Prior to use, the capillary was treated with 0.1 M NaOH and doubly distilled water for 10 min each. Subsequently, the capillary was filled with the running buffer and conditioned for at least 10 min at the voltage of 12 kV between the two ends of the capillary. CE was performed at a separation voltage of 12 kV. The potential applied to the detection electrode was +0.80 V (*vs.* Ag/AgCl wire electrode). Samples were injected electrokinetically into the capillary at 12 kV for 6 s. The amperometric detector was on during the injection procedures.

3. Results and discussion

3.1. SEM images

In this work, a novel method based on the in situ polymerization of MMA was developed for the facile preparation of graphene/PMMA composite electrode. The graphene/PMMA composite electrode were directly fabricated in the bore of a 320 μm I.D. and 450 μm O.D. fused silica capillary due to the size compatibility of the electrode and the outlet of the separation capillary (25 μm I.D. and 360 μm O.D.), providing an simple way to prepare the detection electrodes for CE. To investigate the surface morphology of PMMA sheet, graphenes, and the cross sections of graphene/PMMA and graphite/PMMA composites, their scanning electron microscopy (SEM) images were measured (Fig. 1). Obviously, the surface morphology of graphene/PMMA composite was much different from that of pristine graphenes because the PMMA in the composite could adhere graphenes to form an interconnected graphene network. A great amount of edges of graphenes were observed on the surface of graphene/PMMA composite, indicating graphenes were well dispersed and connected in the composite. This graphene network may establish electric conduction pathways throughout the whole system, which is responsible for the electric conductivity and electrochemical sensing. Fig. 1d shows the SEM image of the cross section of graphite/PMMA composite. Obviously, graphite plates can be observed.

3.2. XRD patterns and FT-IR spectra

Fig. 2 displays XRD patterns of graphene, graphene/PMMA composite, and PMMA. Diffraction peaks assigned to graphenes at 24.2° and 42.9° (corresponding to the indices of (0 0 2) and (1 0 0)) [9] can be clearly seen for both pure graphene and graphene/PMMA composite, indicating that the graphene structure was not destroyed after the in situ polymerization of MMA. The three broad characteristic peaks of PMMA were also observed in the XRD pattern of graphene/PMMA composite, while the second peak of graphenes merges with the third peak of PMMA.

FT-IR spectra of graphene, graphene/PMMA composite and pristine PMMA (Fig. 3) were also measured. In the IR spectra of pristine PMMA and graphene/PMMA composite, the absorption bands at 2994 cm^{-1}, 2951 cm^{-1}, 1732 cm^{-1}, and in the ranges of 1365–1484 cm^{-1} and 1149–1273 cm^{-1} were assigned to CH_3, CH_2, C=O, C–H, and C–O–C, respectively [37]. All of the characteristic peaks of PMMA and graphene can be found in the FT-IR spectrum of the graphene/PMMA composite. Some of these peaks overlap, meaning that their relative heights and shapes change to some extent in comparison with the IR spectra of pristine PMMA and graphene.

3.3. Thermogravimetry of graphene/PMMA composite

Thermogravimetry was employed to evaluate the weight fraction of graphene in the graphene/PMMA composite. Fig. 4 shows the TGA and DTGA curves of graphene and the graphene/PMMA composite at a heating rate of 10 °C/min. Obvious weight loss of the composite was found in the temperature ranges of 216–376 °C and 500–655 °C due to the decomposition of PMMA and graphene, respectively. Based on the TGA curve, the weight fraction of graphenes was estimated to be approximately 25% (w/w) that was well in agreement with the expected value. In comparison with graphene/PMMA composite, pristine graphene starts to degrade around 370 °C and decomposes almost completely at 580 °C, indicating that the thermal stability of graphene in the composite was significantly enhanced.

3.4. CE conditions

To demonstrate the feasibility and performance of the graphene/PMMA composite electrode, it was coupled with a CE system as an end-column amperometric detector for the separation and detection of rutin, hyperin, kaempferol, corilagin, geraniin, gal-

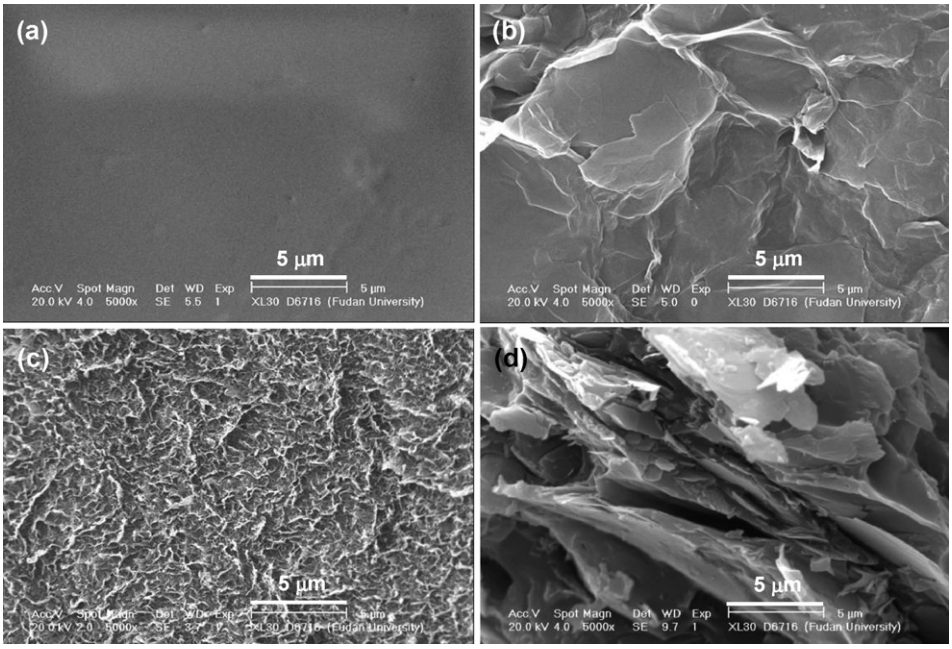

Fig. 1. SEM images of pristine PMMA sheet (a), graphene (b), and the cross sections of graphene/PMMA (c) and graphite/PMMA composites. Conditions: accelerating voltage, 20 kV; magnification, 5000×.

lic acid, and protocatechuic acid. In order to enhance the resolution and solubility of the analytes, alkaline borate buffer was employed in this study. The seven analytes are partially negatively charged in alkaline borate buffer because their phenolic hydroxy and carboxylic groups can dissociate to form anions. In this work, 50 mM borate buffer (pH 9.2) was chosen as the running buffer considering peak current, resolution, analytical time, and its buffering capacity. The separation voltages (12 kV) were the same as the injection voltage for convenience. In addition, samples were introduced into the capillary electrokinetically. The optimum injection time was 6 s (at 12 kV), considering the separation and sensitivity.

3.5. Current responses and detection limits of the analytes after CE separation

Fig. 5 illustrates the representative electropherograms of a mixture containing 50 μg/mL rutin, 50 μg/mL hyperin, 50 μg/mL kaempferol, 50 μg/mL corilagin, 100 μg/mL geraniin, 200 μg/mL gallic acid, and 200 μg/mL protocatechuic acid at graphite/PMMA and graphene/PMMA composite electrodes. The seven analytes could be separated resulting in well-defined and resolved peaks within 13 min when the graphene-based composite electrode was used. As shown in Fig. 5, the peak currents of the seven analytes at the graphene/PMMA composite electrode are much higher than those at the graphite/PMMA composite detector. The sharpness of the peaks decreased apparently in CE when the graphite/PMMA composite detector was used, indicating the phenolic compounds strongly adsorbed on the graphite in the composite. The current responses of rutin, hyperin, kaempferol, corilagin, geraniin, gallic

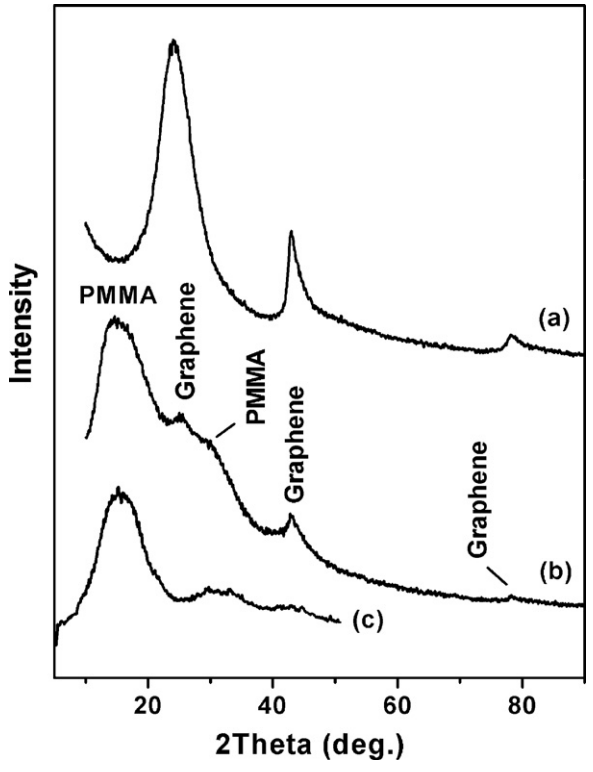

Fig. 2. XRD patterns of graphene (a), graphene/PMMA composite (b), and PMMA (c).

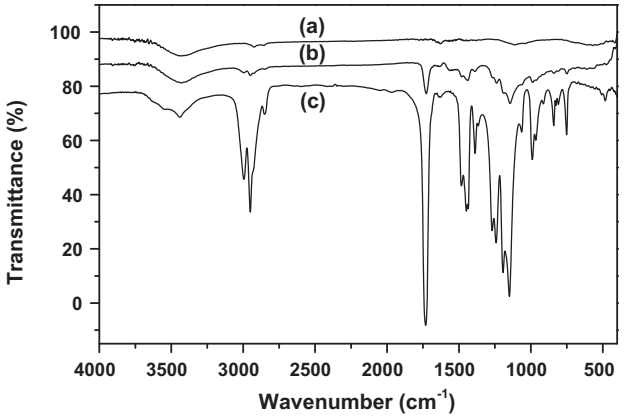

Fig. 3. FT-IR spectra of graphene (a), graphene/PMMA composite (b), and PMMA (c).

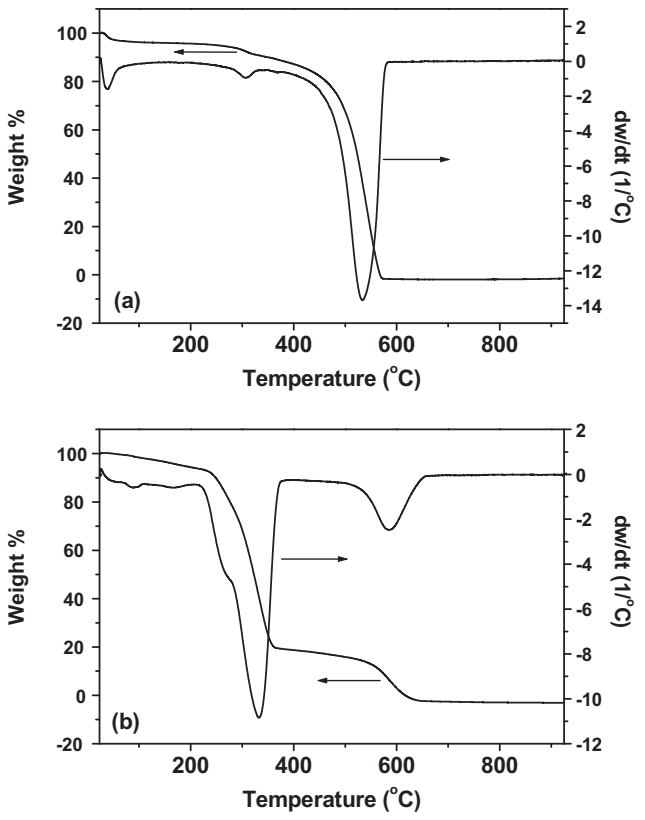

Fig. 4. GA and DTGA curves of graphene (a) and graphene/PMMA composite (b).

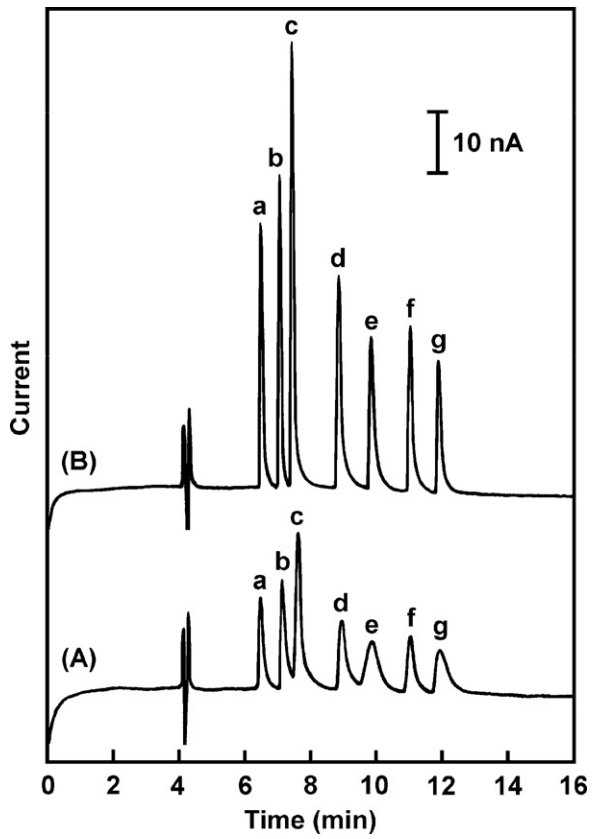

Fig. 5. Electropherograms for a mixture containing 50 μg/mL rutin (a), 50 μg/mL hyperin (b), 50 μg/mL kaempferol (c), 50 μg/mL corilagin (d), 100 μg/mL geraniin (e), 200 μg/mL gallic acid (f), and 200 μg/mL protocatechuic acid (g) at (A) graphite/PMMA and (B) graphene/PMMA composite electrodes. Conditions: used-silica capillary, 25 μm I.D. × 40 cm length; detection electrode, 320 μm diameter disc electrode; running buffer, 50 mM borate buffer (pH 9.2); separation and injection voltage, 12 kV; injection time, 6 s, detection potential, 0.8 V (*vs.* Ag/AgCl wire electrode).

acid, and protocatechuic acid were 41.3, 48.5, 69.3, 33.1, 23.6, 25.8 and 20.7 nA at the graphene/PMMA composite electrode and 14.0, 17.3, 23.4, 11.1, 7.2, 8.8 and 6.6 nA at the graphite/PMMA composite electrode, respectively. The higher responses of the graphene-based composite detector led to lower detection limits compared to the graphite-based electrode [36.3 *vs.* 107.0, 30.9 *vs.* 86.8, 21.6 *vs.* 63.9, 45.3 *vs.* 135.6, 126.9 *vs.* 416.8, 232.2 *vs.* 682.8, and 290.1 *vs.* 910.3 μg/L for rutin, hyperin, kaempferol, corilagin, geraniin, gallic acid, and protocatechuic acid, respectively (based on $S/N = 3$)]. The detection limit of rutin at the graphene/PMMA composite electrode is much better than that measured using a carbon disk electrode that was made of a graphite pencil rod [36]. Recently, a graphene/poly(urea-formaldehyde) composite modified electrode was developed in our laboratory based on the polycondensation of a mixture of graphene and urea-formaldehyde prepolymer on the surface of a platinum disk electrode. The sensitivity and detection limits of the graphene/PMMA composite electrode are comparable with those of the graphene/poly(urea-formaldehyde) composite modified electrode [12]. Overall, the graphene/PMMA composite is a promising material for electrochemical sensing. The present graphene/PMMA composite electrode shows higher signal-to-niose ratio and stable baseline. In addition, higher voltage resulted in shorter migration time for all compounds, but also increased the baseline noise, resulting in poorer detection limits. In this work, the separation voltage was 12 kV, considering resolution and signal-to-noise ratio. When the separation voltage was higher than 12 kV, hyperin and kaempferol could not be baseline resolved.

3.6. Hydrodynamic voltammograms (HDVs)

Fig. 6 depicts the HDVs for the oxidation of 50 μg/mL corilagin at graphite/PMMA and graphene/PMMA composite electrodes. The curves were recorded point-wise over the +0.1 to +1.1 V (*vs.* Ag/AgCl electrode) range by changing the applied potential by 0.1 V. The current response of the graphene-based composite electrode was higher than that of the graphite/PMMA composite electrode at the same potential. When the applied potential exceeded +0.50 V for the graphite/PMMA and +0.30 V for the graphene/PMMA composite electrodes, the peak current of both electrodes raised rapidly. However, the current responses increased much slowly upon increasing

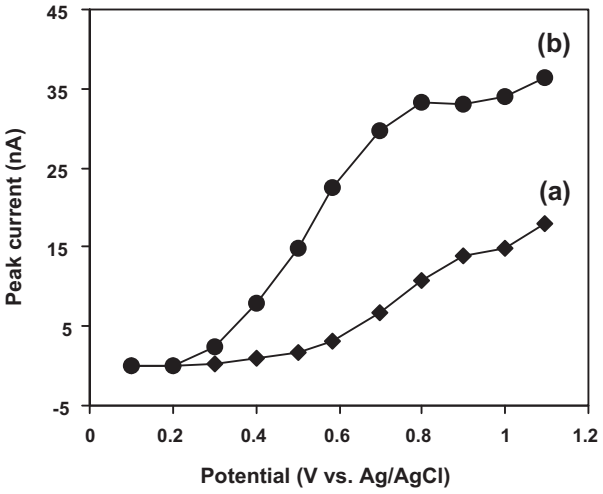

Fig. 6. Hydrodynamic voltammograms for 50 μg/mL corilagin at graphite/PMMA (a) and graphene/PMMA (b) composite electrodes. Conditions as in Fig. 5.

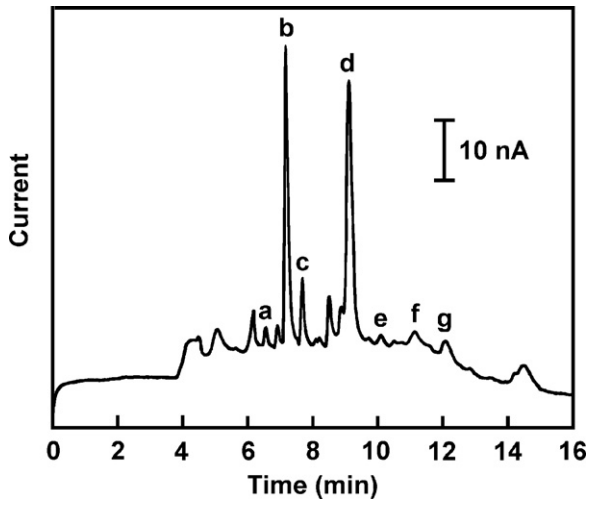

Fig. 7. Typical electropherogram for the diluted extracts from a sample of *Herba Geranii*. Peak labels and other conditions as in Fig. 5.

the potential above +0.90 V and +0.80 V for the graphite/PMMA and the graphene/PMMA composite electrodes, respectively. In this work, the applied potential of the graphene-based electrode was maintained at +0.80 V. At this detection potential, the background current was not too high and the signal-to-noise ratio was the highest. The half-wave potentials at the graphite/PMMA and the graphene/PMMA composite electrodes were +0.70 and +0.52 V for corilagin. The electrocatalytic activity toward the investigated analyte was pronounced as the half-wave potential on the graphene/PMMA composite electrode decreased by 180 mV in comparison with that on the graphite/PMMA composite electrode, indicating that the graphene-based electrode allowed amperometric detection with higher sensitivity and at significantly lower detection potentials. It was reported that the ability of graphenes to promote electron-transfer reactions on the electrode could be attributed to their special electronic structure and high electric conductivity [9–12]. As shown in Fig. 1c, the edges of graphenes on the surface of the graphene/PMMA composite work like thousands upon thousands microelectrodes. The mass transfer on the conducting graphene network was significantly enhanced so that the current response was enhanced.

3.7. Linearity range, day-to-day and intraday reproducibility of detection

A series of the standard mixture solutions of the seven analytes with concentration ranging from 0.5 to 500 μg/mL were tested to determine the linearity range at the graphene/PMMA composite electrode. The results indicated that the graphene-based electrode displays a well-defined concentration dependence. Nine determinations of a mixture containing 50 μg/mL rutin, 50 μg/mL hyperin, 50 μg/mL kaempferol, 50 μg/mL corilagin, 100 μg/mL geraniin, 200 μg/mL gallic acid, and 200 μg/mL protocatechuic acid over 3 days (three times a day) resulted in the day-to-day signal reproducibilities of 4.1, 3.7, 3.6, 3.9, 4.2, 4.4, and 4.7%, respectively. The intraday reproducibility was examined from a series of eight repetitive injections of the same standard mixture solution under the selected conditions. Reproducible signals were obtained with relative standard deviations (RSDs) of 3.5% (rutin), 3.2% (hyperin), 2.9% (kaempferol), 3.4% (corilagin), 3.8% (geraniin), 3.7% (gallic acid), and 4.0% (protocatechuic acid) for the peak currents. Such good repeatability reflects the reduced surface fouling of the graphene/PMMA composite electrode, indicating that this approach is suitable for the analysis of real samples.

3.8. Sample analysis

In addition, the suitability of the graphene-based detector to real plant samples was demonstrated by determining seven naturally occurring phenolic constituents in *Herba Geranii* (a traditional Chinese medicine) after CE separation. Fig. 7 illustrates the electropherogram of a diluted extract of *Herba Geranii* in the running buffer. The contents of rutin, hyperin, kaempferol, corilagin, geraniin, gallic acid, and protocatechuic acid in the herbal drug were determined to be 0.02569 (*RSD* 4.1%, $n = 3$), 0.3307 (*RSD* 2.6%, $n = 3$), 0.05319 (*RSD* 3.9%, $n = 3$), 0.4180 (*RSD* 2.1%, $n = 3$), 0.05128 (*RSD* 4.3%, $n = 3$), 0.1134 (*RSD* 3.2%, $n = 3$), and 0.2051 (*RSD* 2.7%, $n = 3$) mg/g that that were similar to the data in a previous report [30]. The results demonstrated that this method had both high accuracy and good precision for the analytes measured in the real sample.

4. Conclusions

In summary, a new approach based on in situ polymerization has been developed for the fabrication of graphene/PMMA composite electrode as the end-column amperometric detector of CE. The performance, the utility, and the advantages of the novel setup have been demonstrated in combination with the separation and detection of seven naturally occurring phenolic compounds in *Herba Geranii*. It is characterized by its higher resolution and sensitivity, lower expense of operation, and less amount of sample. The novel graphene-based CE detector offers favorable signal-to-background characteristics, strong electrocatalytic activity, sharp peaks for the analytes and simple design and fabrication, indicating great promise for a wide range of applications.

Acknowledgments

This work was financially supported by NSFC (20875015 and 21075020), the State Oceanic Administration (201105007), the Ministry of Science and Technology (2006BAI19B02), Shanghai Science Committee (2009JC1401400), and the Education Ministry of China (NCET-08-0134).

References

[1] K.S. Novoselov, A.K. Geim, S.V. Morozov, D. Jiang, Y. Zhang, S.V. Dubonos, I.V. Grigorieva, A.A. Firsov, Science 306 (2004) 666.
[2] C.N.R. Rao, A.K. Sood, K.S. Subrahmanyam, A. Govindaraj, Angew. Chem. Int. Ed. 48 (2009) 7752.
[3] M. Pumera, Chem. Rec. 9 (2009) 211.
[4] A. Ambrosi, T. Sasaki, M. Pumera, Chem. Asian J. 5 (2010) 266.
[5] C. Shan, H. Yang, J. Song, D. Han, A. Ivaska, L. Niu, Anal. Chem. 81 (2009) 2378.
[6] M. Zhou, Y.M. Zhai, S.J. Dong, Anal. Chem. 81 (2009) 5603.
[7] Y.Y. Shao, J. Wang, H. Wu, J. Liu, I.A. Aksay, Y.H. Lin, Electroanalysis 22 (2010) 1027.
[8] C.K. Chua, A. Ambrosi, M. Pumera, Electrochem. Commun. 13 (2011) 517.
[9] Y. Wang, Y.M. Li, L.H. Tang, J. Lu, J.H. Li, Electrochem. Commun. 11 (2009) 889.
[10] J.F. Wu, M.Q. Xu, G.C. Zhao, Electrochem. Commun. 12 (2010) 175.
[11] H.F. Xu, H. Dai, G.N. Chen, Talanta 81 (2010) 334.
[12] B. Chen, L.Y. Zhang, G. Chen, Electrophoresis 32 (2011) 870.
[13] J.W. Jorgenson, K.D. Lukacs, Anal. Chem. 53 (1981) 1298.
[14] J.W. Jorgenson, K.D. Lukacs, J. Chromatogr. 218 (1981) 209.
[15] R.A. Frazier, A. Papadopoulou, Electrophoresis 24 (2003) 4095.
[16] C.C. Lin, Y.T. Li, S.H. Chen, Electrophoresis 24 (2003) 4106.
[17] C.W. Huck, G. Stecher, H. Scherz, G. Bonn, Electrophoresis 26 (2005) 1319.
[18] B. Baena, A. Cifuentes, C. Barbas, Electrophoresis 26 (2005) 2622.
[19] G. Chen, Y.Z. Zhu, Y.F. Wang, X.J. Xu, T. Lu, Curr. Med. Chem. 13 (2006) 2467.
[20] L.A. Holland, A.M. Leigh, Electrophoresis 23 (2002) 3649.
[21] G. Chen, Talanta 74 (2007) 326.
[22] A.G. Crevillen, M. Pumera, M.C. Gonzalez, A. Escarpa, Electrophoresis 29 (2008) 2997.
[23] A.G. Crevillen, Monica Avila, M. Pumera, M.C. Gonzalez, A. Escarpa, Anal. Chem. 79 (2007) 7408.
[24] B.G. Wei, J. Wang, Z. Chen, G. Chen, Chem. Eur. J. 14 (2008) 9779.
[25] G. Chen, L.Y. Zhang, J. Wang, Talanta 64 (2004) 1018.
[26] B.G. Wei, P.P. Guan, L.Y. Zhang, G. Chen, Carbon 48 (2010) 1380.

[27] B.G. Wei, L.Y. Zhang, G. Chen, New J. Chem. 34 (2010) 453.
[28] D.C. Shin, D.A. Tryk, A. Fujishima, A. Muck, G. Chen, J. Wang, Electrophoresis 25 (2004) 3017.
[29] Committee of National Pharmacopoeia, Pharmacopoeia of People's Republic of China, vol. 1, Chinese Medical Science and Technology Press, Beijing, 2010, p. 113.
[30] X. Jin, F. Wang, L. Yao, Q.Y. Wu, Q.L. Wang, L.F. Liu, Chin. Trad. Patent Med. 32 (2010) 1172.
[31] G. Chen, J.H. Li, S. Qu, D. Chen, P.Y. Yang, J. Chromatogr. A 1094 (2005) 138.
[32] G.X. Xu, J. Wang, Y. Chen, L.Y. Zhang, D.R. Wang, G. Chen, Lab Chip 6 (2006) 145.
[33] K.P. Pramoda, H. Hussain, H.M. Koh, H.R. Tan, C.B. He, J. Polym. Sci. 48 (2010) 4262.
[34] S. Villar-Rodil, J.I. Paredes, A. Martınez-Alonso, J.M.D. Tascón, J. Mater. Chem. 19 (2009) 3591.
[35] C.M. Chen, Q.H. Yang, Y.G. Yang, W. Lv, Y.F. Wen, P.X. Hou, M.Z. Wang, H.M. Cheng, Adv. Mater. 21 (2009) 3007.
[36] G. Chen, H.W. Zhang, J.N. Ye, Anal. Chim. Acta 423 (2000) 69.
[37] K. Awazu, H. Onuki, J. Non-Crys. Sol. 215 (1997) 176.